

First-principles calculations of hyperfine interactions in La_2CuO_4

P. Hüsser, H. U. Suter, E. P. Stoll, and P. F. Meier

Physics Institute, University of Zurich, CH-8057 Zurich, Switzerland

(Received 3 May 1999; revised manuscript received 23 July 1999)

We present the results of first-principles cluster calculations of the electronic structure of La_2CuO_4 . Several clusters containing up to nine copper atoms embedded in a background potential were investigated. Spin-polarized calculations were performed both at the Hartree-Fock level and with density-functional methods with generalized-gradient corrections to the local-density approximation. The distinct results for the electronic structure obtained with these two methods are discussed. The dependence of the electric-field gradients at the Cu and the O sites on the cluster size is studied and the results are compared to experiments. The magnetic hyperfine coupling parameters are carefully examined. Special attention is given to a quantitative determination of on-site and transferred hyperfine fields. We provide a detailed analysis that compares the hyperfine fields obtained for various cluster sizes with results from additional calculations of spin states with different multiplicities. From this we conclude that hyperfine couplings are mainly transferred from nearest-neighbor Cu^{2+} ions and that contributions from further distant neighbors are marginal. The mechanisms giving rise to transfer of spin density are worked out. Assuming conventional values for the spin-orbit coupling, the total calculated hyperfine interaction parameters are compared with those derived from experiments.

I. INTRODUCTION

A large amount of information about both static and dynamic properties of materials that exhibit high-temperature superconductivity, is available through experimental techniques like nuclear quadrupole and magnetic resonances (NQR and NMR). In particular, the electric-field gradients have been determined for a variety of nuclei with great accuracy.¹ These quantities are ground-state properties of the solid and depend sensitively on how charge is shared among the atomic and molecular orbitals. Measurements of the Knight shift and the various nuclear relaxation rate tensors as a function of temperature, doping, and orientation of the applied field with respect to the crystalline axes, provide insight into the static spin-density distribution and the low-frequency spin dynamics of the electrons in the normal as well as in the superconducting state.² Owing to the abundances of nuclei with suitable nuclear magnetic and quadrupole moments, most of these quantities can be studied on different sites in the unit cell. This allows one to distinguish static and dynamic features in the CuO_2 planes from those in the interlayer region.

The analysis of numerous early NQR and NMR experiments focused on the question whether a one-component model is sufficient to describe the low-energy excitations of the quantum fluid in the high-temperature superconductors or whether a two-component description is needed. Knight shift and relaxation rate data for the Cu sites in $\text{YBa}_2\text{Cu}_3\text{O}_7$ that were analyzed on the basis of the hyperfine coupling of a Cu^{2+} ion in an axial symmetric surrounding, seemed to be controversial. Mila and Rice³ proposed then that besides the usual on-site hyperfine interactions at a Cu nucleus an additional hyperfine field should be considered which is transferred from neighboring Cu ions. They gave a consistent explanation of the unusual combination of anisotropies of the Cu Knight shifts and relaxation rates in $\text{YBa}_2\text{Cu}_3\text{O}_7$ within a one-component theory. An estimation of the strength of the

various hyperfine parameters with the use of a quantum chemical model led to good agreement with the values deduced from experiment. Monien, Pines, and Slichter⁴ analyzed a more complete set of data from which they inferred the relevant hyperfine couplings and the associated fluctuation times. The ensuing constraints on theoretical one-component models for the planar magnetic excitations comprise a large transferred hyperfine field between adjacent Cu^{2+} spins, which, moreover, must be very nearly aligned antiferromagnetically, and, in addition, an almost perfect cancellation between the parallel component of the dipolar hyperfine tensor and the total transferred field ($A_{\parallel} + 4B \approx 0$). Provided that the spin susceptibility is isotropic, it is only with the latter condition that the vanishing of the parallel component of the spin contributions to the Knight shift can be explained.

A remaining intricate problem whose explanation seemed to require a two-band model, was the relaxation behavior of the planar oxygen nuclei which was strikingly different from that of the coppers. Shastry,⁵ however, pointed out that spin density is also transferred to the planar oxygens. A transferred hyperfine field couples a nucleus to spin fluctuations on neighboring Cu sites. This implies that the spin-lattice relaxation time T_1 depends on form factors given by the local geometry of lattice sites of the nucleus and its neighbors. Since the form factor entering $^{17}\text{T}_1$ vanishes at the commensurate antiferromagnetic wave vector $(\pi/a, \pi/a)$ where that for $^{63}\text{T}_1$ reaches a maximum, the variant temperature dependence of $^{17}\text{T}_1$ and $^{63}\text{T}_1$ could be understood from the presence of strong antiferromagnetic correlations between the copper spins in the planes. Thus a coherent picture of the low-energy spin dynamics in the CuO_2 planes seemed to be established⁶ and numerous NMR and NQR experiments were analyzed on the basis of these hyperfine spin Hamiltonians and a one-band model. Pines and co-workers developed⁷ a phenomenological expression for the dynamic

spin susceptibility and provided^{8,9} a quantitative description of a variety of NMR data.

Doubts about the adequacy of a one-component description of the spin fluid arose when the results of neutron-scattering data became available. NMR and neutrons both probe the spin susceptibility. In $\text{La}_{1.86}\text{Sr}_{0.14}\text{CuO}_4$, a considerable degree of incommensuration of the peaks in the spin-fluctuation spectrum was observed.¹⁰ As a consequence, the NMR relaxation time $^{17}T_1$ is expected to exhibit an anomalous temperature dependence which is not seen experimentally. This and other contradictions between the results of NMR and neutron-scattering experiments led Zha, Barzykin, and Pines¹¹ to a critical re-examination of the hyperfine spin Hamiltonian. They showed that it is possible to reconcile NMR and neutron-scattering experiments on both $\text{La}_{2-x}\text{Sr}_x\text{CuO}_4$ and $\text{YBa}_2\text{Cu}_3\text{O}_{6+x}$ within a one-component theory by introducing a transferred hyperfine coupling between the O nuclei and their next-nearest-neighbor Cu^{2+} spins. In addition, the analysis exhibited that the hyperfine coupling transferred to the Cu nuclei changes as one goes from the $\text{La}_{2-x}\text{Sr}_x\text{CuO}_4$ to the $\text{YBa}_2\text{Cu}_3\text{O}_{6+x}$ system, and is moreover comparatively sensitive to hole doping in the former system.

Despite the rich information of NMR and NQR results about the nature of the spin fluid and the low-energy quasiparticles, there exist only few theoretical first-principles approaches which address the determination of electric-field gradients and magnetic hyperfine interactions. For the $\text{YBa}_2\text{Cu}_3\text{O}_{6+x}$ system, electric-field gradients (EFG's) at the various nuclear sites have been obtained by Das and co-workers¹²⁻¹⁴ with *ab initio* cluster calculations using the unrestricted Hartree-Fock (UHF) method, and by Schwarz and co-workers^{15,16} who employed the full-potential linear augmented-plane-wave method within the local-density approximation (LDA). Results of Hartree-Fock (HF) calculations have also been published by Winter.¹⁷ Apart from one exception, the EFG's calculated with these three different methods more or less agree and reproduce the experimental data quite satisfactorily. The exceptional case is the EFG at the planar Cu sites. Using a large cluster that contained 74 atoms, we recently performed¹⁸ calculations with the density-functional (DF) method and obtained values for the Cu EFG's which are in better agreement with the experiments. These calculations were nonspin polarized and no information on magnetic hyperfine interactions is available. The energy difference between the singlet and triplet states of two coppers in adjacent CuO_2 planes was studied¹⁹ in a small cluster containing two Cu, four Y, and eight O atoms.

For the La_2CuO_4 system, UHF calculations have been reported by Sulaiman *et al.*²⁰ who obtained EFG values at various nuclei as well as the contact and dipolar hyperfine fields at Cu. Martin and Hay²¹ presented HF results of the electronic structure of CuO_6 clusters in neutral, *p*-doped, and *n*-doped states and studied the influence of correlation effects using the technique of configuration interactions. Martin²² calculated HF values for EFG's in CuO_6 and Cu_2O_{11} clusters and investigated the change in the NQR spectra upon doping. A comparison²³ of HF and LDA calculations for a CuO_6 cluster showed large differences in the EFG values and the hyperfine coupling parameters.

In this paper, the results of extensive cluster studies for

the pure La_2CuO_4 system are presented. Spin-polarized calculations at the HF level and with the DF method with gradient corrections to the correlation functionals have been performed for clusters comprising $n=1, 2, 4, 5,$ and 9 Cu atoms in a plane. The resulting electronic structures, the charge and spin distributions, EFG's and magnetic hyperfine interactions have been analyzed. In Sec. II, details on the clusters, their embedding in a lattice of point charges, the basis sets and the theoretical methods are given. Results for the $(\text{CuO}_6)^{10-}$ ion are presented in Sec. III and compared to the predictions for the hyperfine couplings of a Cu^{2+} ion in a single-electron picture. The distinct results of HF and DF methods are discussed in detail. Section IV is devoted to the investigation of the EFG values for Cu and the planar and apical oxygens and their dependence on the cluster size. The results for the magnetic hyperfine interactions are given in Sec. V. Particular emphasis is put on investigations of contributions to the hyperfine fields transferred from nearest and further distant copper ions. The origins of the various hyperfine couplings are worked out and explained in terms of localized atomic orbitals and molecular orbitals. The general mechanisms giving rise to spin-density transfer are discussed. Sec. VI contains a summary and conclusions.

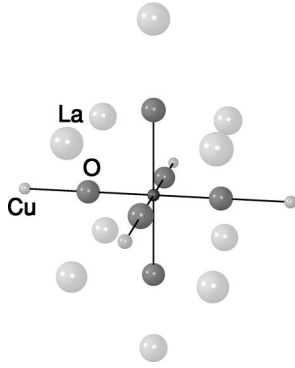
II. CLUSTERS AND BASIS SETS

The general idea of the cluster approach to electronic structure calculations is that the parameters that characterize a small cluster should be transferable to the solid and largely determine its properties. The essential contributions to EFG's and to magnetic hyperfine fields are given by rather localized interactions and therefore it is expected that these local properties can be determined and understood with clusters calculations. Approximations must be made concerning the treatment of the background that is employed to embed the cluster. Using as large a cluster as is possible is of course advantageous. It is necessary, however, that the results obtained should be checked with respect to their dependence on the cluster size.

The clusters used in this work comprise copper atoms of the CuO_2 plane together with the surrounding planar and apical oxygens. They were embedded in a lattice of point charges with charges $+2, -2,$ and $+3$ according to the ionic charges of $\text{Cu}^{2+}, \text{O}^{2-},$ and La^{3+} , respectively. However, it has been pointed out in Ref. 21 that bare positive point charges close to the border of the cluster present a too strong attraction for the electrons. It is, therefore, essential to replace them by appropriate pseudopotentials which guarantee the orthogonality of the diffuse electron wave functions with the ion cores.

The smallest cluster investigated is shown in Fig. 1. All-electron basis sets were put on one Cu and six O atoms and pseudopotentials were used to represent the four Cu^{2+} and ten La^{3+} sites closest to the cluster border. In addition, these 21 atoms were surrounded by more than 2000 point charges. Some charges at sites far from the cluster center were adjusted such that the total charge of the system was zero. Next, the positions of some point charges were changed in such a way that the correct Madelung potential in the central region of the cluster was reproduced.

All atomic positions were located according to the tetrag-

FIG. 1. The $\text{CuO}_6/\text{Cu}_4\text{La}_{10}$ cluster.

onal phase with lattice constants²⁴ $a = 3.77 \text{ \AA}$ and $c = 13.18 \text{ \AA}$ and with a Cu-O(a) distance of 2.40 \AA .

For the cluster atoms the standard 6-311G basis sets were employed. For Cu, this corresponds to the basis set developed by Wachters,²⁵ while for O it was given in Ref. 26. In Table I an overview is presented of the clusters used in this work with a listing of the numbers of Cu atoms, of cluster atoms, of electrons, of basis functions, and of primitive Gaussian functions.

The majority of the HF and DF calculations were spin polarized. They were performed with the GAUSSIAN94 and GAUSSIAN98 programs.²⁷ The Vosko-Wilk-Nussair functional²⁸ (VWN) was used as local-density approximation (LDA). For the gradient corrections to the exchange and correlation functionals several forms for the generalized-gradient approximations (GGA) are available in the literature. As in our investigations¹⁸ on $\text{YBa}_2\text{Cu}_3\text{O}_7$, we mainly used the formula proposed by Becke^{29,30} in combination with the functional of Lee, Yang, and Parr³¹ (BLYP). For the smallest cluster, other functionals have been used as well, such as the X_α -LYP (XALYP) and the form proposed by Perdew and Wang.³² (BPW91). The individual integrals over the atomic orbitals for the electric-field gradient were taken from calculations using the GAMESS-US program.³³ For the final analysis a special program was designed³⁴ which employed these integrals and the electronic wave functions from the Gaussian calculations.

Throughout this work we use atomic units for the electric-field gradients and magnetic hyperfine interaction parameters. To distinguish these from other notations, we will use lower case letters and write, e.g., the hyperfine spin Hamiltonian for a nuclear spin I and a single electron spin S as

$$H = \sum_{\alpha\beta} I_\alpha A_{\alpha\beta} S_\beta = \hbar \gamma_I \hbar \gamma_e \sum_{\alpha\beta} I_\alpha a_{\alpha\beta} S_\beta. \quad (1)$$

TABLE I. Clusters, number of atoms N , atoms with pseudopotentials PP, total number of electrons E , number of basis functions B , and number of primitive Gaussian functions P .

Cluster	N	PP	E	B	P
CuO_6	7	$\text{Cu}_4\text{La}_{10}$	87	117	222
Cu_2O_{11}	13	$\text{Cu}_6\text{La}_{12}$	164	221	418
Cu_4O_{20}	24	$\text{Cu}_8\text{La}_{26}$	308	334	772
Cu_5O_{26}	31	$\text{Cu}_8\text{La}_{34}$	395	533	1006
Cu_9O_{42}	51	$\text{Cu}_{12}\text{La}_{50}$	663	897	1686

TABLE II. EFG component V_{zz} , core polarization a_{cp} , dipolar contribution to the hyperfine tensor $a_{\text{dip}}^{\parallel}$, and atomic spin density ρ at the Cu, as obtained with HF and DF/GGA calculations for the cluster $\text{CuO}_6/\text{Cu}_4\text{La}_{10}$.

Method	Basis	V_{zz}	a_{cp}	$a_{\text{dip}}^{\parallel}$	ρ
HF ^a		2.232	-0.503	-4.421	0.88
HF ^b		1.840			
HF	6-311G	1.936	-3.519	-4.421	0.902
DF/BLYP	6-311G	1.419	-1.784	-3.526	0.667

^aReference 20.

^bReference 22.

The tensor $a_{\alpha\beta}$ has the dimension of a density. In the NMR literature, different and sometimes misleading units are in use. We note that $2\mu_B/a_B^3 = 125.2 \text{ kG}$, which connects to the units used in Ref. 4.

III. EMBEDDED CuO_6 ION

To investigate the $(\text{CuO}_6)^{-10}$ ion embedded in an environment of the La_2CuO_4 system, the cluster $\text{CuO}_6/\text{Cu}_4\text{La}_{10}$ shown in Fig. 1 was used. The results for the EFG component V_{zz} , the core polarization a_{cp} , the dipole tensor $a_{\text{dip}}^{\parallel}$, and the atomic spin density ρ at the Cu site are collected in Table II.

Our results for V_{zz} and $a_{\text{dip}}^{\parallel}$ obtained at the HF level agree with previous calculations.^{20,22} There exist, however, distinct differences between the HF results and those calculated within the DF/GGA scheme. In HF, the EFG's are about 40% larger than those obtained from DF calculations. A similar discrepancy between EFG values calculated with HF and DF methods has also been observed¹⁸ in calculations of the EFG at the planar Cu site in the $\text{YBa}_2\text{Cu}_3\text{O}_7$ system.

The calculated results are not sensitive if different exchange and correlation functionals in the DF approach are used. This will be shown in Sec. V A together with results obtained by using other basis sets.

The experimental value³⁵ of the quadrupole frequency at the ^{63}Cu is 33.0 MHz. This corresponds to $V_{zz} = 1.331$ assuming a quadrupole moment $Q(^{63}\text{Cu}) = -0.211 \text{ b}$. A more detailed comparison between experimental and theoretical values for the EFG is given in Sec. IV. The results for the core polarization and the dipole tensor will be discussed in Sec. V.

It is instructive to compare these *ab initio* results for the embedded $(\text{CuO}_6)^{10-}$ ion with the predictions for a single-electron (or rather single-hole) picture of the Cu^{2+} ion which have been given by Bleaney *et al.*³⁶ If the d shell is full except for a singly occupied $3d_{x^2-y^2}$ orbital, the dipolar hyperfine field is given by

$$a_{\text{dip}}^{\parallel} = -\frac{4}{7} \langle r^{-3} \rangle \quad (2)$$

and the core polarization is determined by a parameter κ :

$$a_{\text{cp}} = -\kappa \langle r^{-3} \rangle. \quad (3)$$

The spin-orbit coupling will be discussed later.

TABLE III. Contributions to the EFG component V_{zz} , calculated with DF/GGA for the cluster $\text{CuO}_6/\text{Cu}_4\text{La}_{10}$, from the nuclei within the cluster, from the point charges around the cluster, and from the individual shells. The “remainder” lists just the (small) rest of all other contributions that cannot be assigned to a particular shell.

Nuclei		0.375	
point charges		0.012	
	Spin up	Spin down	Sum
p_x, p_y	-1.183	-1.210	-2.393
p_z	0.384	0.386	0.770
$d_{x^2-y^2}, d_{xy}$	-9.443	-5.720	-15.163
$d_{3z^2-r^2}$	4.446	4.381	8.827
d_{xz}, d_{yz}	4.522	4.481	9.003
Remainder	0.027	-0.039	-0.012
Total			1.419

Inserting the DF value $a_{\text{dip}}^{\parallel} = -3.526$ from Table II into Eq. (1) gives $\langle r^{-3} \rangle = 6.171$. Using this number and $a_{\text{cp}} = -1.784$ in Eq. (2) leads to $\kappa = 0.289$. The corresponding HF values yield $\langle r^{-3} \rangle = 7.737$ and $\kappa = 0.455$.

Compared with the density-functional *ab initio* results for the embedded $(\text{CuO}_6)^{-10}$ ion, the single-hole picture already gives reasonable results for a_{dip} and a_{cp} . It fails, however, in its prediction of the EFG with a value of $V_{zz} = -4/7\langle r^{-3} \rangle$. This discrepancy has sometimes been used to assign a fractional hole number to the $3d_{x^2-y^2}$ orbital. The underlying physical picture, however, is completely misleading since the contributions to the EFG originate from various Cu shells as can be seen in Table III. The cluster EFG value of 1.4 as obtained with the DF method, results from cancellations between relatively large individual contributions. This shows that the theoretical determination of EFG's is quite delicate. It is necessary to describe all electron shells of the atom accurately.

At this point we would like to discuss the differences in the results as obtained in HF versus DF theory by analyzing the details of the electronic structure. For each spin projection there exists a total of 23 molecular orbitals (MO's) that can be formed as linear combinations of the Cu $3d$ and the six O $2p$ atomic orbitals (AO's). Both HF and DF predict that the MO with highest energy is the antibonding hybridization between Cu $3d_{x^2-y^2}$ and O $2p_x$ and $2p_y$ AO's. It is occupied for one spin projection (spin up) only and, in the following, energies will be measured with respect to the energy of this highest occupied molecular orbital (HOMO). (The HOMO calculated with DF for a cluster comprising nine Cu atoms will be shown in Fig. 5.) The corresponding spin-down orbital is the lowest unoccupied molecular orbital (LUMO) and lies at an energy which is at 1.4 eV for DF and even higher for HF. The energies of all 23 MO's are shown in Fig. 2 together with the contributions from the individual AO's. The length of the bars marks the squared values of the expansion coefficient of the MO with respect to the AO's whereby spin-up (spin-down) orbitals are denoted by solid (dotted) bars.

The orbitals with second highest energy are antibonding linear combinations of the AO's $3d_{3z^2-r^2}$ of the Cu and O

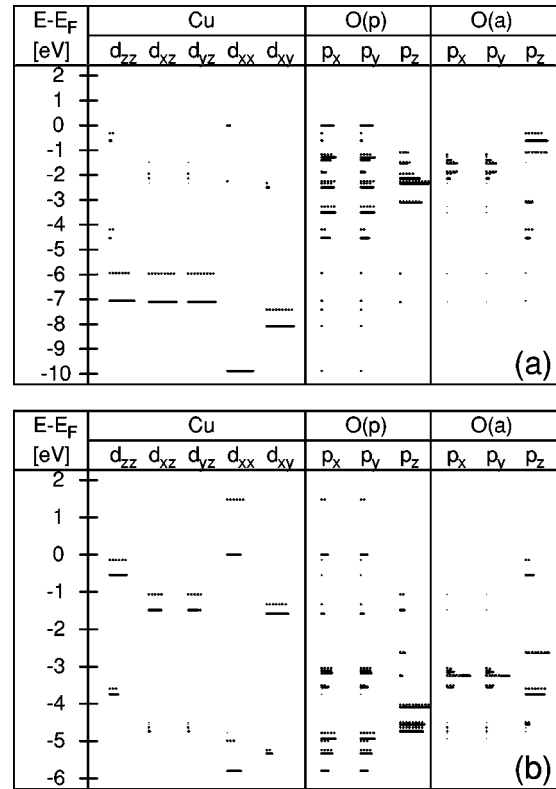


FIG. 2. Energies of the highest occupied MO's in the $\text{CuO}_6/\text{Cu}_4\text{La}_{10}$ cluster with contributions from the individual AO's: (a) HF, (b) DF. The length of the bar is proportional to the square of the expansion coefficient of the MO into the corresponding AO's. Spin-up (spin-down) orbitals are denoted by solid (dashed) bars.

$2p_z$ of the apical oxygens. In the DF calculation, these are followed at energies around -1.5 eV by MO's that can be formed as antibonding hybridizations with the three other Cu $3d$ AO's. Deeper in energy, between -2.6 and -4.4 eV, are the MO's that are composed of oxygens only without contributions from Cu. They comprise the $2p_z$ AO's of the planar oxygens and the $2p_x$ and $2p_y$ of the apex oxygens. At the HF level, these are at energies (-1.1 to -1.8 eV) that are above those of the MO's with contributions from Cu $3d_{xy,yz,zx}$.

The MO with lowest energy in Fig. 2 is at -5.8 eV for DF. It is formed by the bonding hybridization between $3d_{x^2-y^2}$ and O $2p_x$ and $2p_y$. Further down in energy lie 2×21 orbitals formed by inner-shell AO's. Their energies and wave functions are only slightly different for the two spin projections though it is precisely this difference that will determine the core polarization and also contributes to the electric-field gradient. Therefore, it is essential to describe also inner-shell electrons with basis sets of sufficiently high quality.

The HF result suggests an almost purely ionic bonding with small overlap between Cu and O. In contrast, the DF results emphasize the covalent character of the bonds and an appreciable overlap. This variant description of bonding is also reflected in the width of the “ d band” (10 eV vs 6 eV) and the localization of the atomic spin density at the Cu (0.90 vs 0.67).

The contributions of the DF MO's shown in Fig. 2 to the density of states is represented in Fig. 3. The individual

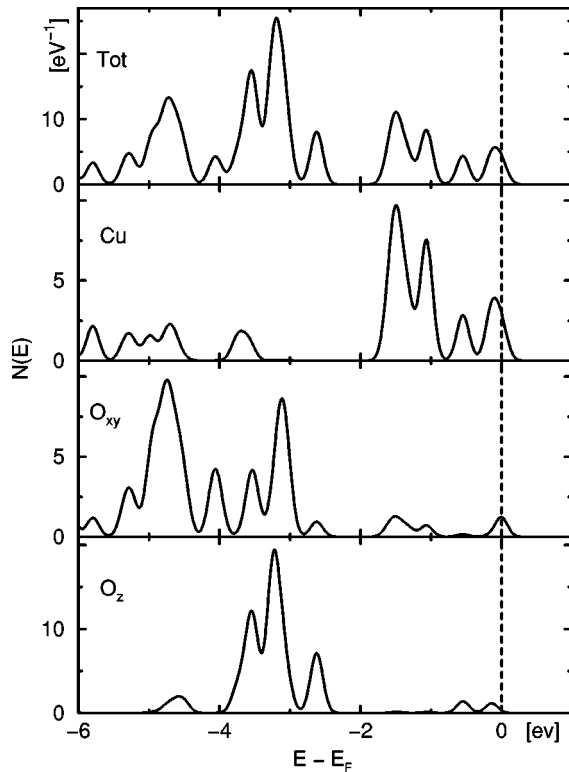


FIG. 3. Total and partial density of states of the highest ‘‘band’’ in the $\text{Cu}_9\text{O}_{42}/\text{Cu}_{12}\text{La}_{50}$ cluster as obtained with the DF method.

states were broadened by folding with a Gaussian function of half-width 0.21 eV. A comparison to the density of states obtained from band-structure calculations^{37,38} shows an overall agreement even for the small cluster under consideration.

The total occupation of the DF Cu atomic orbitals amounts to 8.96 which results from the following contributions: 0.04, 0.91, 0.97, 0.97, 0.94, 0.96 from $4s$, $3d_{3z^2-r^2}$, $3d_{zx}$, $3d_{yz}$, $3d_{x^2-y^2}$, $3d_{xy}$ with spin up and 0.05, 0.91, 0.96, 0.96, 0.33, 0.96 with spin down. The small population of the Cu $4s$ AO is due to the fact that the hybridization between the $3d_{3z^2-r^2}$ and the $2p_z$ of the apex oxygens also involves a minor admixture of $4s$ orbitals. The populations obtained from the analysis of the HF results are somewhat higher, in agreement with Sulaiman *et al.*²⁰

In conclusion, we think that the Cu-O bonding is better described by DF methods, which include part of the correlation, than with HF. This will gain further evidence from the results obtained with larger clusters that will be reported in the following sections.

IV. ELECTRIC-FIELD GRADIENTS

A. Larger clusters

To investigate the convergence of the calculated EFG’s and magnetic hyperfine properties with respect to cluster size, calculations for clusters comprising n Cu atoms ($n = 1, 2, 4, 5, 9$) have been performed using the HF method as well as DF with GGA (BLYP functional). The multiplicity m of the spin states was chosen to be maximal ($m = 2n + 1$). Lower multiplicities were also investigated for selected clusters ($m = 0$ for $n = 2$ and $m = 2, 4$ for $n = 5$). On all atoms belonging to the cluster, a 6-311G basis set was employed.

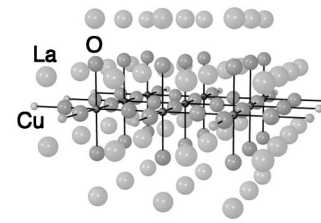


FIG. 4. The $\text{Cu}_9\text{O}_{42}/\text{Cu}_{12}\text{La}_{50}$ cluster.

In Fig. 4 the largest cluster used is represented. It comprises nine Cu and 42 O atoms in the plane and is surrounded by 12 Cu and 50 La ions that were treated with bare pseudopotentials. The corresponding HOMO as obtained with DF methods is shown in Fig. 5. In this section, the resulting EFG values are discussed whereas the magnetic hyperfine properties will be analyzed in Sec. V.

B. Electric-field gradients at the Cu site

The results of Hartree-Fock and density-functional calculations for the V_{zz} component of the EFG at the Cu site are given in Table IV. Since the Cu sites in the two clusters with even number of Cu atoms are not situated in the center, a small asymmetry η results. Again, the large discrepancy between HF and DF results is obvious. Our HF values for small clusters are in agreement with those obtained in Refs. 20,22.

The variations of the values for the EEG’s with respect to cluster size and multiplicity are within reasonable bounds considering the subtle cancellations of contributions from the various shells as can be seen in Table III.

The experimental value³⁵ for the ^{63}Cu quadrupole frequency is 33.0 MHz. This corresponds to a value for V_{zz} of 1.331 a.u. using a quadrupole moment of $^{63}Q = -0.211$ b, but to 1.560 a.u. with $^{63}Q = -0.18$ b. The former value for ^{63}Q is from an analysis of Sternheimer³⁹ and is the one cited in the current NQR tables while the latter was determined by Stein *et al.*⁴⁰ from a HF cluster calculation for cuprite. In relation to the large amount of NQR data available on cuprate superconductors, the availability of reliable values for the quadrupole moments of Cu would be very desirable.

In a comparison with experiments it should further be noted that our calculations were performed for clusters with atomic positions corresponding to the tetragonal phase. Moreover, spin states with lower multiplicities better account for antiferromagnetic fluctuations than high-spin states. In this respect, our calculated values are by 17% too low, even

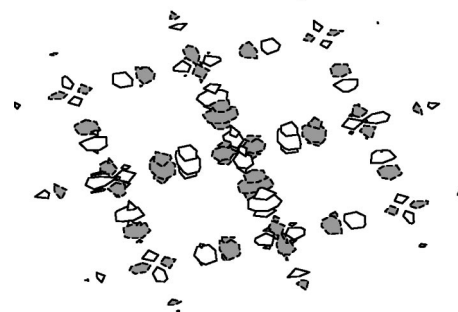


FIG. 5. Highest occupied molecular orbital for the $\text{Cu}_9\text{O}_{42}/\text{Cu}_{12}\text{La}_{50}$ cluster.

TABLE IV. EFG component V_{zz} and asymmetry parameter η for the Cu site in the La_2CuO_4 system calculated for different cluster sizes and various spin multiplicities m . The basis set used for all calculations was 6-311G. For comparison, the theoretical results of Sulaiman *et al.* (Ref. 20) and Martin (Ref. 22), as well as the measured quadrupole frequency (Ref. 49), have been transformed into EFG values.

Cluster	m	HF		LDA/GGA	
		V_{zz}	η	V_{zz}	η
$\text{CuO}_6/\text{Cu}_4\text{La}_{10}$	2	1.936	0	1.419	0
$\text{Cu}_2\text{O}_{11}/\text{Cu}_6\text{La}_{12}$	3	1.939	0.06	1.380	0.22
$\text{Cu}_2\text{O}_{11}/\text{Cu}_6\text{La}_{12}$	1	1.884	0.04	1.260	0.21
$\text{Cu}_4\text{O}_{20}/\text{Cu}_8\text{La}_{26}$	5	1.925	0.00	1.354	0.01
$\text{Cu}_5\text{O}_{26}/\text{Cu}_8\text{La}_{34}$	6	1.963	0	1.128	0
$\text{Cu}_5\text{O}_{26}/\text{Cu}_8\text{La}_{34}$	4			1.071	0
$\text{Cu}_5\text{O}_{26}/\text{Cu}_8\text{La}_{34}$	2			1.097	0.28
$\text{Cu}_9\text{O}_{42}/\text{Cu}_{12}\text{La}_{40}$	10	1.975	0	1.264	0
CuO_6^a		2.234	0.02		
$\text{CuO}_6/\text{Cu}_4\text{La}_{10}^b$		1.840			
$\text{Cu}_2\text{O}_{11}/\text{Cu}_6\text{La}_{12}^b$		1.816			
Experiment ^c		1.560($^{63}\text{Q} = -0.18b$)		1.331($^{63}\text{Q} = -0.211b$)	

^aReference 20.

^bReference 22.

^cReference 35.

with $^{63}\text{Q} = -0.211b$. Nevertheless, it can be concluded that a valuable estimate for V_{zz} can already be gained with DF calculations with the cluster $\text{CuO}_6/\text{Cu}_4\text{La}_{10}$. This is of relevance for studies of the changes in the quadrupole frequency upon doping.

C. Electric-field gradients at the O site

Although the clusters used in this report were constructed to investigate mainly the magnetic hyperfine interactions at the Cu site, the results obtained for the EFG's at the oxygen sites are also of interest. For the planar oxygen O(p) they are listed in Table V. Again, we find reasonable agreement between the experimental values and our calculations with the DF method.

For O(a), the apical oxygen, the EFG is axially symmetric and the component V_{zz} turned out to have the values 0.26,

TABLE V. EFG components for the planar oxygen O(p).

Cluster	HF			LDA/GGA		
	V_{xx}	V_{yy}	V_{zz}	V_{xx}	V_{yy}	V_{zz}
$\text{Cu}_2\text{O}_{11}/\text{Cu}_6\text{La}_{12}$	-0.430	0.334	0.096	-0.889	0.525	0.364
$\text{Cu}_4\text{O}_{20}/\text{Cu}_8\text{La}_{26}$	-0.403	0.363	0.040	-0.839	0.536	0.303
$\text{Cu}_5\text{O}_{26}/\text{Cu}_8\text{La}_{34}$	-0.411	0.326	0.049	-0.847	0.545	0.302
$\text{Cu}_9\text{O}_{42}/\text{Cu}_{12}\text{La}_{50}$	-0.499	0.353	0.146	-0.881	0.554	0.327
Experiment ^a	-0.75	0.51	0.24	-0.75	0.51	0.24

^aReference 41.

TABLE VI. EFG component V_{zz} , core polarization a_{cp} , dipolar contribution to the hyperfine tensor $a_{\text{dip}}^{\parallel}$, and atomic spin density ρ at the Cu, as obtained with DF/GGA calculations for the cluster $\text{CuO}_6/\text{Cu}_4\text{La}_{10}$ for various basis sets and functionals.

Method	Basis	V_{zz}	a_{cp}	$a_{\text{dip}}^{\parallel}$	ρ
DF/BLYP	6-311G	1.419	-1.784	-3.526	0.667
DF/BLYP	6-311Gpd	1.360	-1.784	-3.502	0.661
DF/BLYP	uncontracted	1.508	-1.627	-3.596	0.669
DF/SVWN	6-311G	1.364	-1.625	-3.425	0.642
DF/XALYP	6-311G	1.367	-1.801	-3.409	0.635
DF/BPW91	6-311G	1.415	-1.943	-3.517	0.669

0.21, and 0.19 for DF (0.28, 0.26, and 0.19 for HF) for clusters with four, five, and nine Cu atoms, respectively. The experimental value⁴¹ is 0.22.

V. CORE-POLARIZATION AND TRANSFERRED HYPERFINE FIELDS

A. Isotropic contributions

The magnetic hyperfine interaction at a nucleus can be separated into an isotropic part D and a traceless dipolar part. The former is given by the difference between the spin densities at the nuclear site R :

$$D(R) = \frac{8\pi}{3} \left(\sum_m |\psi_m^\uparrow(R)|^2 - \sum_{m'} |\psi_{m'}^\downarrow(R)|^2 \right), \quad (4)$$

where the sums extend over all occupied MO's. This quantity is called Fermi contact interaction. Strictly it arises from the spin density at a nucleus but there are two ways, direct and indirect, that this can happen if we use an "atoms in molecules" approach. The direct way is either from occupancy of s -like atomic orbitals centered on the nucleus or any other orbital centered on a remote nucleus, the latter normally being a very small contribution. The indirect mechanism is usually via a core-polarization process where an unpaired spin is located in a non- s -like valence orbital which spin polarizes the core s -like electrons.

It should be noted that the core-polarization term is notoriously difficult to compute accurately compared to the EFG or the dipolar hyperfine interaction parameters since it is crucially dependent on the correct treatment of electron correlation. For molecules, this has been investigated extensively, and Cu species in particular have been studied by Barone.⁴²⁻⁴⁴ For our smallest cluster, we have performed additional calculations with various density functionals (SVWN, XALYP, BPW91) and basis sets including the 222 basis functions of the 6-311G set but all uncontracted. The results which are compiled in Table VI agree among each other reasonably well. Increasing the quality of the basis set by including polarization (p) and diffuse (d) functions also does not alter the results substantially.

The variations in the values for the core-polarization term due to approximations such as inadequate basis set or inappropriate choice functional, should clearly be distinguished from the changes that depend on the transfer of spin density from neighboring Cu^{2+} ions which were all obtained with

TABLE VII. Atomic spin densities and D values at different planar sites in the cluster $\text{Cu}_9\text{O}_{42}/\text{Cu}_{12}\text{La}_{50}$ as obtained with the DF method. N denotes the number of nearest-neighbor Cu ions.

Position	N	ρ	D
Cu(0/0)	4	0.6935	0.9215
Cu(2/0)	3	0.6870	0.3209
Cu(2/2)	2	0.6766	-0.3636
O(1/0)	2	0.1427	1.2550
O(2/1)	2	0.1390	1.2214
O(3/0)	1	0.0896	0.6501
O(3/2)	1	0.0815	0.6384

the same (contracted) 6-311G basis set. To emphasize this difference we used for the core-polarization the notation a_{cp} for the single Cu atom but $D(\text{Cu})$ for clusters with several copper atoms.

The values for $D(\text{Cu})$ vary strongly with cluster size and position of a particular Cu atom in larger clusters. In the $\text{Cu}_9\text{O}_{42}/\text{Cu}_{12}\text{La}_{40}$ cluster, e.g., $D=0.922$ for the central Cu which is surrounded by four nearest neighbors (NN), but $D=-0.364$ at the four equivalent corner sites which have 2 NN and $D=0.321$ at the four sites on the edges with 3 NN. The complete set of data is compiled in Table VII. In Fig. 6, the values for $D(\text{Cu}_i)$ obtained with clusters of different sizes are plotted vs N , the number of nearest-neighbor Cu atoms of Cu_i . In all calculations, the same basis set 6-311G was used. It is obvious that in a first approximation the increase of $D(\text{Cu})$ is linear in the number of nearest-neighbor Cu atoms for both DF and HF methods. It is suggestive to attribute this change to a transferred hyperfine term b and to separate $D(\text{Cu})$ into

$$D(\text{Cu}) = a + bN \quad (5)$$

with preliminary values: $a \approx -1.75$ and $b \approx 0.69$ for DF/BLYP and $a \approx -3.52$ and $b \approx 0.17$ for HF.

For those oxygen sites that are at the border of the cluster and that are therefore bounded to a single Cu atom, a value

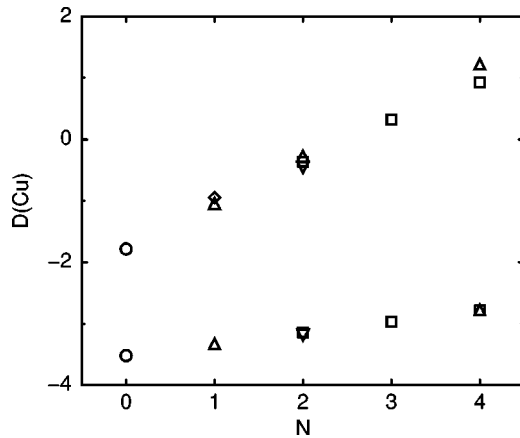


FIG. 6. Difference between spin-up and -down densities at Cu vs number of nearest-neighbor Cu atoms N for different sites in various clusters with n Cu atoms. Circles: $n=1$, diamonds: $n=3$, triangle down: $n=4$, triangle up: $n=5$, squares: $n=9$. DF (HF) values correspond to the upper (lower) data set.

$D(\text{O}) \approx 0.64$ is found. For oxygens bridging two Cu atoms, however, we get $D(\text{O}) \approx 1.24$ with the HF values 0.60 and 1.11 being only slightly lower. Therefore, also the core polarization at O is determined by a transferred hyperfine field from its neighboring Cu atoms:

$$D(\text{O}) = cN \quad (6)$$

with a preliminary value $c \approx 0.6$.

At the apex oxygens, the spin density is marginal (on the order of 1%) and the core polarization amounts to 0.05.

In retrospect, some of the early problems in analyzing NQR and NMR data on cuprate superconductors can be traced back to the fact that the single-hole model developed in Ref. 36 for an isolated Cu^{2+} ion in a crystal field, cannot be applied to correlated Cu ions in a CuO_2 plane. To be precise, it works reasonably well for local quantities like the dipolar coupling tensor and the spin-orbit interaction which will be discussed later. Their values are mainly determined by the HOMO and also do not depend too sensitively on the method of treating the many-electron system. Even HF calculations give results of the correct order of magnitude. The core polarization, however, is not a local affair. As Fig. 6 exhibits, hyperfine fields transferred from the neighboring copper ions have a drastic effect on $D(\text{Cu})$. Its value is negative for an isolated copper ion but is increased by contributions from neighboring ions. At the HF level, there is a small hybridization and the transfer is small. DF calculations, however, render a stronger covalency and therefore the spin density is more delocalized which implies a larger transfer. With contributions from four NN Cu ions, $D(\text{Cu})$ becomes positive as was first recognized by Mila and Rice.³

The question then arises whether also contributions from further distant Cu atoms will contribute to the hyperfine properties at Cu or O. This is of particular relevance since to reconcile NMR and neutron-scattering experiments within a one-component spin model, Zha *et al.*¹¹ have advocated a hyperfine field at oxygen transferred from second nearest Cu neighbors. This would lead to a reduction of the form factor $^{17}F(\vec{q})$ around the wave vector $\vec{q} = (\pi/a, \pi/a)$ and to a modification of the spin-lattice relaxation rate $^{17}T_1^{-1}$.

To investigate this problem of hyperfine fields transferred from further distant neighbors in detail, we performed also DF cluster calculations for spin states with lower multiplicity. In the cluster $\text{Cu}_5\text{O}_{26}/\text{Cu}_8\text{La}_{34}$ states with multiplicities $m=4$ and $m=2$ were obtained. For the former the spin density at the central Cu atom is of opposite sign to that of the four neighboring sites. For $m=2$, it is negative at the central and one edge Cu atom. In Fig. 7 the corresponding differences in the spin densities along the Cu-O-Cu-O-Cu axes are shown. They peak at positions where the squares of the $3d_{x^2-y^2}$ orbitals have their maxima. The core polarization then yields a change close to the Cu nucleus. In the ‘‘antiferromagnetic’’ cluster that is obtained with $m=4$, the atomic spin density at the central Cu is negative but its magnitude is smaller than those at the four adjacent coppers (the detailed results are given in Table VIII). This is due to the finite size of the cluster. There is an excess of positive spin density in the central region which is also reflected by the atomic spin densities at the four oxygens that are bridging

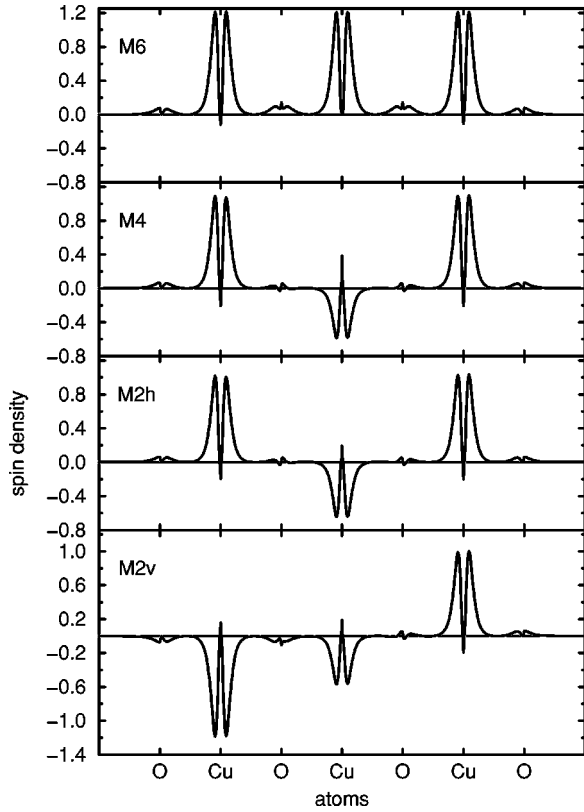


FIG. 7. Difference in spin densities along the O-Cu-O-Cu-O-Cu-O bonds as calculated with DF/GGA for the cluster $\text{Cu}_5\text{O}_{26}/\text{Cu}_8\text{La}_{34}$. From top to bottom: multiplicity $m=6$, $m=4$, and $m=2$ horizontally (vertically) with spin-density signs $+-+$ ($--+$).

two antiferromagnetically coupled Cu atoms. There, a value of 0.026 is obtained instead of the cancellation expected for a large system.

To account for these finite-size effects, we have carefully analyzed all results given in Tables VII and VIII. It turned out that the values of the core polarization at the oxygens are

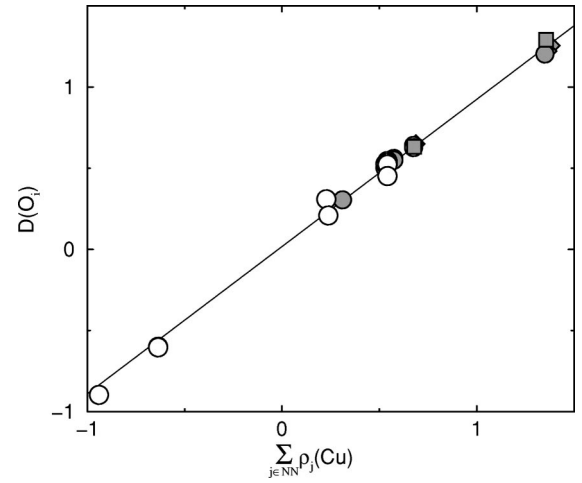


FIG. 8. Difference between spin-up and -down densities at O(p) vs sum of atomic spin densities at neighboring Cu atoms for different sites in various clusters: Cu_9 (diamonds), Cu_5 , $m=6$, and $m=4$ (circles), Cu_4 (squares), and Cu_5 with $m=2$ (open circles).

proportional to the sum of atomic spin densities at the adjacent Cu ions

$$D(\text{O}) = \gamma \sum_{j \in \text{NN}} \rho(\text{Cu}_j), \quad (7)$$

where the sum extends over one or two NN. This is illustrated in Fig. 8. The negative values result from the spin states with lower multiplicities. The deviations from the linear behavior for some small $D(\text{O})$ values is due to errors in forming the difference between large $\rho(\text{Cu}_j)$ values with opposite signs.

Similarly, the core polarization at the Cu ions can well be reproduced by separating it according to

$$D(\text{Cu}_i) = \alpha \rho(\text{Cu}_i) + \beta \sum_{j \in \text{NN}} \rho(\text{Cu}_j). \quad (8)$$

TABLE VIII. Atomic spin densities and D values at different planar sites in the cluster $\text{Cu}_5\text{O}_{26}/\text{Cu}_8\text{La}_{34}$ as obtained for spin multiplicities $m=6$, 4, and 2 with the DF method.

Position	$m=6$		$m=4$		$m=2$	
	ρ	D	ρ	D	ρ	D
Cu(0/0)	0.6745	1.1963	-0.2636	3.2337	-0.3036	1.5959
Cu(2/0)	0.6743	-0.9500	0.5738	-1.7329	0.5412	-1.6747
O(1/0)	0.1356	1.2034	0.0260	0.3062	0.0199	0.2086
O(3/0)	0.0818	0.6258	0.0726	0.5500	0.0677	0.5228
O(2/1)	0.0872	0.6417	0.0705	0.5603	0.0660	0.4520
Cu(0/2)					-0.6364	1.3237
Cu(0/-2)					0.5310	-1.6093
O(0/1)					-0.0893	-0.8956
O(0/3)					-0.0778	-0.6023
O(0/-1)					0.0143	0.3083
O(0/-3)					0.0697	0.5043
O(1/2)					-0.0773	-0.5994
O(2/-1)					-0.0651	0.5345
O(1/-2)					0.0657	0.5265

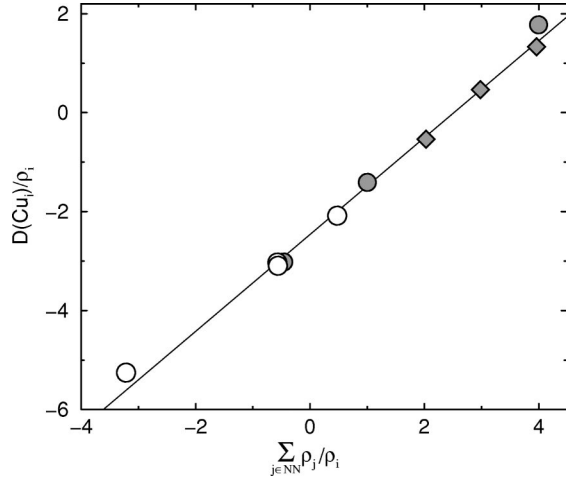


FIG. 9. $D(\text{Cu}_i)/\rho(\text{Cu}_i)$ values plotted against the sum of atomic spin densities at the NN Cu atoms divided by $\rho(\text{Cu}_i)$: Cu_9 (diamonds), Cu_5 , $m=6$ and $m=4$ (circles), and Cu_5 with $m=2$ (open circles).

In Fig. 9 the various values $D(\text{Cu}_i)/\rho(\text{Cu}_i)$ are plotted as a function of the sum of NN atomic spin densities divided by $\rho(\text{Cu}_i)$.

With all these data available, we are now in a position to study the intrinsic and transferred hyperfine fields in a quantitative manner and to estimate also the influence of next-nearest and further distant Cu atoms. The isotropic hyperfine constants at the oxygens were assumed to depend on the spin densities of the adjacent (NN), next-nearest-neighbors (NNN) and further distant Cu atoms according to

$$D(\text{O}) = \gamma \sum_{j \in \text{NN}} \rho(\text{Cu}_j) + \gamma' \sum_{j \in \text{NNN}} \rho(\text{Cu}_j) + \gamma'' \sum_{j \in \text{NNNN}} \rho(\text{Cu}_j). \quad (9)$$

For Cu, the isotropic hyperfine constants were decomposed into

$$D(\text{Cu}_i) = \alpha \rho(\text{Cu}_i) + \beta \sum_{j \in \text{NN}} \rho(\text{Cu}_j) + \beta' \sum_{j \in \text{NNN}} \rho(\text{Cu}_j) + \beta'' \sum_{j \in \text{NNNN}} \rho(\text{Cu}_j). \quad (10)$$

Figures 8 and 9 already show that the main contributions are due to NN. This result is corroborated by least-squares fits of all data to Eqs. (9) and (10) which yield

$$\alpha = -2.54 \pm 0.04, \quad \beta = 1.02 \pm 0.02, \\ |\beta'| \leq 0.02, \quad |\beta''| \leq 0.02 \quad (11)$$

and

$$\gamma = 0.925 \pm 0.006, \quad |\gamma'| \leq 0.006, \quad |\gamma''| \leq 0.006. \quad (12)$$

As expected, the contributions from Cu ions beyond NN are marginal.

The analyses performed so far have demonstrated that all hyperfine coupling parameters are proportional to the sum of

TABLE IX. Values for the dipolar hyperfine couplings for Cu and O(p) for different clusters.

Cluster	$a_{\text{dip}}^{\parallel}(\text{Cu})$		$c_{\text{dip}}^{\parallel}(\text{O})$	
	HF	DF	HF	DF
$\text{CuO}_6/\text{Cu}_4\text{La}_{10}$	-4.421	-3.526	0.181	0.388
$\text{Cu}_2\text{O}_{11}/\text{Cu}_6\text{La}_{12}$	-4.431	-3.480	0.332	0.686
$\text{Cu}_4\text{O}_{20}/\text{Cu}_8\text{La}_{26}$	-4.452	-3.479	0.322	0.656
$\text{Cu}_5\text{O}_{26}/\text{Cu}_8\text{La}_{34}$	-4.486	-3.249	0.324	0.668
$\text{Cu}_9\text{O}_{42}/\text{Cu}_{12}\text{La}_{40}$	-4.491	-3.370	0.324	0.684

the atomic spin densities at the adjacent Cu ions. The essential point is that in this way also the values calculated for lower spin multiplicities could be accounted for. These contain complementary informations to the results of high-spin states which strongly improve the quality of the results as can be seen in Figs. 8 and 9. Incorporating negative values of $\sum_j \rho(\text{Cu}_j)$ into the evaluation renders a much better understanding of the various contributions.

We are now in a position to extrapolate the data from the finite clusters to an extended system. Considering the three different values of $\rho(\text{Cu}_i)$ in the largest cluster (see Table VII), we expect $\rho(\text{Cu})$ in the homogeneous case to be 0.70.

This leads to the following values: $a = -1.778$, $b = 0.714$, $|b'| \leq 0.014$, $c = 0.648$, and $|c'| \leq 0.004$.

It should be emphasized again that the extracted values for the contact terms depend on the particular choice of the exchange-correlation functional and the basis set. We have performed a few calculations with other functionals, too. They deliver values that differ by 15% but they also lead to the conclusion that contributions from further distant neighbors are not important.

B. Dipolar hyperfine interactions

In contrast to the core polarization, which is proportional to the spin-density difference at a single point, the dipolar hyperfine coupling results from a spatial average of $1/r^3$ with wave functions. Its value, therefore, can be determined with much greater accuracy than that of the contact interaction and does less crucially depend on the calculational method or the choice of the exchange-correlation functionals. It is given by

$$a_{\text{dip}}^{\text{ij}}(R) = \sum_m \langle \psi_m^{\uparrow}(r) | T^{\text{ij}}(r-R) | \psi_m^{\uparrow}(r) \rangle - \sum_{m'} \langle \psi_{m'}^{\downarrow}(r) | T^{\text{ij}}(r-R) | \psi_{m'}^{\downarrow}(r) \rangle, \quad (13)$$

where

$$T^{\text{ij}}(x) = \frac{3x_i x_j - \delta_{ij} x^2}{x^5}. \quad (14)$$

In Table IX the values for $a_{\text{dip}}^{\parallel}$ (for Cu) and $c_{\text{dip}}^{\parallel}$ (for O) obtained with various clusters are given. It should be remarked that $c_{\text{dip}}^{\parallel}$ for planar oxygen refers to the directions along the Cu-O-Cu bonds. The tensor coupling is only nearly axially symmetric.

TABLE X. Compilation of results for the hyperfine interactions at $O(p)$ and comparison with values extracted from experiments.

	c	$c_{\text{dip}}^{\text{xx}}$	$c_{\text{dip}}^{\text{yy}}$	$c_{\text{dip}}^{\text{zz}}$	$c_{\text{tot}}^{\text{xx}}$	$c_{\text{tot}}^{\text{yy}}$	$c_{\text{tot}}^{\text{zz}}$
Present	0.648	0.369	-0.177	-0.192	1.017	0.471	0.456
$\text{La}_2\text{CuO}_4^{\text{a}}$					0.748	0.480	0.527
$\text{La}_2\text{CuO}_4^{\text{b}}$					0.863	0.511	0.615

^aReference 11.

^bReference 45.

In analogy to the isotropic case, the dipolar contributions also turned out to depend mainly on the atomic spin densities of the NN copper ions besides the on-site term for Cu which is proportional to the on-site atomic spin density. A least-squares fit of all data (including those with lower multiplicities) to the ansatz

$$a_{\text{dip}}^{\parallel}(\text{Cu}_i) = \alpha_{\text{dip}}\rho(\text{Cu}_i) + \beta_{\text{dip}} \sum_{j \in \text{NN}} \rho(\text{Cu}_j) + \beta'_{\text{dip}} \sum_{j \in \text{NNN}} \rho(\text{Cu}_j) + \beta''_{\text{dip}} \sum_{j \in \text{NNNN}} \rho(\text{Cu}_j) \quad (15)$$

gives $\alpha_{\text{dip}} = -5.206 \pm 0.014$, $\beta_{\text{dip}} = 0.101 \pm 0.006$, and $|\beta'_{\text{dip}}| = |\beta''_{\text{dip}}| \leq 0.005$. Thus there is also a small transferred dipolar hyperfine interaction for Cu.

For the oxygens, the ansatz

$$c_{\text{dip}}^{\parallel}(\text{O}) = \gamma_{\text{dip}} \sum_{j \in \text{NN}} \rho(\text{Cu}_j) + \gamma'_{\text{dip}} \sum_{j \in \text{NNN}} \rho(\text{Cu}_j) + \gamma''_{\text{dip}} \sum_{j \in \text{NNNN}} \rho(\text{Cu}_j) \quad (16)$$

leads to $\gamma_{\text{dip}} = 0.527 \pm 0.006$, $|\gamma'_{\text{dip}}| \leq 0.006$, and $|\gamma''_{\text{dip}}| \leq 0.006$.

Performing the same extrapolation as was applied to the isotropic contributions, we finally get $a_{\text{dip}}^{\parallel} = -3.644$, $b_{\text{dip}}^{\parallel} = 0.071$, $c_{\text{dip}}^{\text{xx}} = 0.369$ (along the bond direction), $c_{\text{dip}}^{\text{yy}} = -0.177$ (perpendicular to the bond), and $c_{\text{dip}}^{\text{zz}} = -0.192$ (perpendicular to the plane).

Represented in Table X are the magnetic hyperfine couplings calculated for $O(p)$. The spin-orbit contributions to the hyperfine fields are expected to be small in the case of O. We neglect them completely by assuming $c_{\text{tot}}^{\text{ii}} = c + c_{\text{dip}}^{\text{ii}}$. These values may be compared to those which have been extracted from various experiments in Refs. 11 and 45.

C. Origin of the transferred hyperfine fields

To investigate the mechanisms of spin transfer, we will analyze in detail the results from the two clusters containing one and two copper atoms and point out the differences. We commence by noting that the basic notions of spin-polarized density-functional theory⁴⁶ rely on the concept of expressing all physical relevant quantities in terms of the spin densities alone. The ‘‘wave functions’’ are just auxiliary entities that are introduced to solve the Kohn-Sham equations⁴⁷ and have no direct physical meaning. Nevertheless, to understand the

TABLE XI. Contributions to the core polarization at an oxygen, $D(\text{O})$, with one ($N=1$) adjacent Cu ion, between two ($N=2$) adjacent Cu ions, and difference. The numbers in parentheses are contributions from AO's centered at remote nuclei.

Atomic orbital	$N=1$	$N=2$	Difference
$1s$	-0.141 (0.000)	-0.245 (0.000)	-0.104 (0.000)
$2s$	0.772 (0.012)	1.570 (0.067)	0.798 (0.055)
Total	0.632 (0.012)	1.326 (0.067)	0.694 (0.055)

origins of transferred hyperfine fields, it is convenient to assign the AO's which are built up from localized basis functions to atomic single-electron wave functions. Similarly, the MO's are interpreted as hybridizations between the individual AO's. Another remark concerns the representation of the AO's in terms of basis functions. We recall that the employed basis sets describe a ‘‘single-electron wave function’’ as a linear combination of several contracted radial Gauss functions. For Cu, there are three radial functions for each of the five $3d$ orbitals and nine functions of s -like character. For O, we have four s functions and three radial functions for each of the $2p$ orbitals.

Let us first consider the $(\text{CuO}_6)^{10-}$ ion embedded in the appropriate lattice. Overlap and covalent effects convey spin density from the Cu^{2+} ion onto the ligand oxygen sites whose spin direction is parallel to that of the local Cu moment. The data in Table II show that in the DF calculations the atomic spin density $\rho(\text{Cu})$ is reduced from 1 to 0.667 in favor of a spin-density transfer to the four planar oxygens [$4 \times \rho(O(p)) = 0.328$]. The transfer from the Cu to the $O(p)$ is much less pronounced at the HF level where $\rho(\text{Cu}) = 0.902$. This trend is also reflected in the dipolar hyperfine coupling (see Table IX): $a_{\text{dip}}^{\text{xx}} = 1.763(2.210)$ and $c_{\text{dip}}^{\text{xx}} = 0.388 (0.181)$ for DF (HF) with a total of $a_{\text{dip}}^{\text{xx}} + 2 \times c_{\text{dip}}^{\text{xx}} = 2.539 (2.572)$. The transferred spin density is mainly on the $O 2p_{\sigma}$ orbital, but a small amount also goes to the $O 2s$ which is thus expected to be polarized parallel to the spin density on the Cu. Indeed, we get $D_{2s}(O) = 0.772$, as can be seen in Table XI where the core polarizations $D(\text{O})$ from DF calculations are listed for the individual orbitals. The $2s$ orbital in turn polarizes the $1s$ but with opposite sign ($D_{1s}(O) = -0.141$). Since the MO's are linear combinations of AO's, the contact term may also have contributions that come from a product of an s -like AO centered at the nucleus under consideration with an AO centered at a remote nucleus. These contributions turn out to be small. They are listed separately as numbers in parentheses in Tables XI and XII. On the Cu, the delocalization of spin densities implies the following changes. The MO second highest in energy (at -0.14 eV) is occupied with a spin-down electron. It mainly mixes the Cu $3d_{3z^2-r^2}$ with the $O(a) 2p_z$ but has also some small contributions from the Cu $4s$ and the $O(p) 2p_{\sigma}$ orbitals. The admixture of the $4s$ is larger than that of the following orbital (at -0.58 eV) which has the same symmetry but is occupied with a spin-up electron. These two MO's thus cause the negative value $D_{4s}(\text{Cu}) = -0.650$ (see Table XII). The $4s$ AO in turn polarizes the inner s orbitals. The alternating signs of the $4s$, $3s$, and $2s$ contributions⁴⁸ are a direct consequence of Hund's rule.

TABLE XII. Contributions to the core polarization at a copper $D(\text{Cu})$ with no adjacent Cu ions ($N=0$), with one NN Cu ion, and their difference. The numbers in parentheses are contributions from AO's centered at remote nuclei.

Atomic orbital	$N=0$		$N=1$		Difference	
$1s$	-0.060	(0.000)	-0.057	(0.000)	0.003	(0.000)
$2s$	-3.734	(0.001)	-3.688	(0.002)	0.046	(0.001)
$3s$	2.650	(0.009)	2.621	(0.010)	-0.029	(0.001)
$4s$	-0.650	(0.001)	0.143	(-0.005)	0.793	(-0.006)
Total	-1.794	(0.011)	-0.981	(0.006)	0.813	(-0.005)

We next consider the system consisting of two Cu atoms with parallel moments and with one bridging O (O_{br}) and six planar O (O_1) bonded to one of the Cu only. The DF calculations yield the atomic spin densities $\rho(\text{Cu}) = 0.670$, $\rho(\text{O}_{\text{br}}) = 0.139$, and $\rho(\text{O}_1) = 0.092$. Since the $2p_\sigma$ orbital can only share a maximal amount of hole contribution, the additional transfer of spin density onto the O_{br} is less than twice the value in the CuO_6 system (2×0.082). The missing fraction is added to the six O_1 . More positive spin density, however, can be put on the $2s$ which leads to the total value $D(\text{O}_{\text{br}}) = 1.326$ (see Table XI). The dipolar contributions are $a_{\text{dip}}^{\text{xx}} = 1.740$ and $c_{\text{dip}}^{\text{xx}} = 0.343$. On the Cu atoms, the spin-density distributions in the inner s shells cannot be changed significantly compared to the CuO_6 case since not much redistribution is possible in the inner core. Therefore, the additional positive spin density resides mainly on the $4s$ atomic orbital.

We thus get a coherent picture of the spin-density distributions for a single Cu^{2+} ion surrounded by four planar oxygens and of the additional spin transfers caused by a second copper ion. The interpretation in terms of localized AO's turned out to be helpful for the understanding of the spin densities which are the relevant quantities in density-functional theory. The results of our quantum chemical calculations demonstrate that the spin densities, when attributed to the Cu or to the O, are strongly connected. In the ground

state, there is no reason for advocating a two-component model and we also see little chance that low-energy excited states could change this fact.

D. Spin-orbit coupling

For Cu, the spin-orbit coupling gives an appreciable contribution to the total hyperfine fields, especially in the perpendicular direction since accidentally a and a_{dip}^\perp almost cancel ($a + a_{\text{dip}}^\perp = 0.003$). A calculation of the spin-orbit interaction cannot be carried out at the same level of quality as is possible for the other hyperfine interactions. Therefore, we adopt the values for the isolated Cu^{2+} ion from Ref. 36 in the simplified form used in Ref. 4:

$$a_{\text{so}}^\parallel = -\frac{62}{7}k\langle r^{-3} \rangle \quad (17)$$

and

$$a_{\text{so}}^\perp = -\frac{11}{7}k\langle r^{-3} \rangle \quad (18)$$

with a parameter value $k = -0.044$. With $\langle r^{-3} \rangle = 6.171$, we get $a_{\text{so}}^\parallel = 2.405$ and $a_{\text{so}}^\perp = 0.427$. It should be noted that the uncertainty in the spin-orbit coupling parameter and the excitation energies is comparatively large. Therefore, in Ref. 4 a range of values for k of $\pm 20\%$ was considered.

In Table XIII all our calculated values for the hyperfine coupling parameters for Cu are compiled. The spin-orbit contributions are put in parentheses to emphasize that they are estimated.

No direct experimental information is available on these parameters. They can be determined indirectly from a combination of anisotropic Knight shifts and relaxation rates and the nuclear resonance frequencies in antiferromagnetic compounds. The results of various analyses are shown in Table XIII. Our values are in reasonable agreement with the data.

TABLE XIII. Compilation of results for the hyperfine interactions at Cu and comparison with values extracted from experiments.

	a	b	a_{dip}^\parallel	b_{dip}^\parallel	a_{so}^\parallel	a_{so}^\perp	a_{tot}^\parallel	a_{tot}^\perp
Present	-1.778	0.714	-3.644	0.071	(2.405)	(0.427)	-3.017	0.471
La_2CuO_4 ^a		0.577					-2.955	0.288
La_2CuO_4 ^b		0.607					-1.550	0.447
$\text{YBa}_2\text{Cu}_3\text{O}_7$ ^c	-2.050	0.744	-3.672		2.086	0.289	-3.636	-0.075
$\text{YBa}_2\text{Cu}_3\text{O}_7$ ^d		0.585					-3.115	0.400
$\text{YBa}_2\text{Cu}_3\text{O}_7$ ^e		0.712					-3.010	-0.179
$\text{YBa}_2\text{Cu}_3\text{O}_7$ ^a		0.687					-2.748	0.495
$\text{YBa}_2\text{Cu}_3\text{O}_7$ ^b		0.623					-2.524	0.591

^aReference 11.

^bReference 49.

^cReference 3.

^dReference 4.

^eReference 6.

VI. SUMMARY AND CONCLUSIONS

The electronic structure of La_2CuO_4 has been investigated by first-principles cluster calculations. These have the advantage that local properties can be studied in great detail but usually suffer from a somewhat uncontrolled embedding in the periodic lattice and surface problems. By using a sequence of clusters containing up to nine copper atoms, we have demonstrated which quantities can be evaluated with clusters of modest size.

As concerns the theoretical approximations to treat the many-electron problem in CuO_2 planes, we have shown that distinct differences between the Hartree-Fock and density functional methods exist. From our results we conclude that the former approach, which neglects correlations entirely, is not adequate for cuprate superconducting materials.

We have evaluated the electric-field gradients at the Cu and the O sites for a variety of cluster sizes and spin multiplicities. For both planar and apical oxygens a satisfactory agreement with the experimentally determined quadrupole frequencies was obtained. For copper, a comparison between theoretical and experimental values is hampered by the uncertainty with which the Cu nuclear quadrupole moments are known.

With respect to magnetic hyperfine properties one has to distinguish between the core polarization and the dipolar contributions. The latter can be determined theoretically with good reliability. The former, however, is a quantity whose value is given by subtle cancellations of contributions from various s -like atomic orbitals. Our calculations demonstrated that besides the negative on-site core-polarization for Cu, a sizeable positive contribution transferred from neighboring Cu^{2+} ions exists as has been suggested by Mila and Rice.³

We have investigated this transfer of spin density in detail and found that there is no appreciable contribution from copper ions other than the nearest neighbors. This is the main result of the present work since it has far reaching consequences. In particular, it questions the reconciliation between NMR and neutron-scattering experiments and points out that the disagreements still exist. By introducing a transferred hyperfine coupling between next-nearest-neighbor Cu spins and ^{17}O nuclei spin, Zha *et al.*¹¹ were able to reconcile many

different experiments. We have shown that there is no microscopic justification for the presence of these additional hyperfine couplings. The discrepancies among the data therefore need another explanation.

On the other hand, the results of the analysis of the origins of the calculated hyperfine fields carried out in Sec. V C show that the spin densities on the coppers and oxygens are very tightly connected. This gives strong support for a one-component model of the spin fluid, at least as concerns ground-state properties in pure La_2CuO_4 .

We have reached these conclusions by carrying out extended *ab initio* cluster calculations. One has, of course, to take into consideration that this approach to describe the electronic structure emphasizes local features and is surely far more appropriate for insulating materials than for metals. It would be a big surprise, however, when a tight-binding picture completely failed to reproduce qualitative aspects of a system with itinerant charge carriers. This would shift the problems to a quite different field.

The calculated values for the magnetic hyperfine couplings are in agreement with those extracted from various NMR and NQR experiments if we adopt the conventional estimates for the spin-orbit interaction for the Cu^{2+} ion. In this respect, improved quantum chemical calculations of the spin-orbit coupling would be desirable. Although our results give a small value for the hyperfine field that contributes to the spin part of the Knight shift in the c direction ($a^{\parallel} + 4b + 4b^{\parallel}$), we think that the vanishing of K_s^{\parallel} below T_c in all high-temperature superconductors and with all doping concentrations is still another open problem that deserves further experimental and theoretical consideration.

ACKNOWLEDGMENTS

We express our gratitude to T. A. Claxton for valuable suggestions and critical reading of the manuscript. We acknowledge useful discussions with D. Brinkmann, M. Mali, S. Schafroth, and J. M. Singer. P.F.M. would like to thank C. P. Slichter for enlightening discussions. This work was partially supported by the Swiss National Science Foundation. A major part of the computation was carried out at the national supercomputing center CSCS.

¹For a review, see D. Brinkmann and M. Mali, *NMR Basic Principles and Progress* (Springer, Heidelberg, 1994), Vol. 31, p. 171.

²See, e.g., A. Rigamonti, F. Borsa, and P. Carretta, *Rep. Prog. Phys.* **61**, 1367 (1998).

³F. Mila and T. M. Rice, *Physica C* **157**, 561 (1989).

⁴H. Monien, D. Pines, and C. P. Slichter, *Phys. Rev. B* **41**, 11 120 (1990).

⁵B. S. Shastry, *Phys. Rev. Lett.* **63**, 1288 (1989).

⁶R. E. Walstedt and W. W. Warren, *Science* **248**, 1082 (1990).

⁷A. J. Millis, H. Monien, and D. Pines, *Phys. Rev. B* **42**, 167 (1990).

⁸H. Monien, P. Monthoux, and D. Pines, *Phys. Rev. B* **43**, 275 (1991).

⁹V. Barzykin and D. Pines, *Phys. Rev. B* **52**, 13 585 (1995).

¹⁰T. E. Mason, A. Schröder, G. Aeppli, H. A. Mook, and S. M. Hayden, *Phys. Rev. Lett.* **77**, 1604 (1996).

¹¹Y. Zha, V. Barzykin, and D. Pines, *Phys. Rev. B* **54**, 7561 (1996).

¹²T. P. Das in *Electronic Properties of Solids Using Cluster Methods*, edited by T. A. Kaplan and S. D. Mahanti (Plenum, New York, 1995).

¹³N. Sahoo, S. Markert, T. P. Das, and K. Nagamine, *Phys. Rev. B* **41**, 220 (1990).

¹⁴S. B. Sulaiman, N. Sahoo, T. P. Das, and O. Donzelli, *Phys. Rev. B* **45**, 7383 (1992).

¹⁵K. Schwarz, C. Ambrosch-Draxl, and P. Blaha, *Phys. Rev. B* **42**, 2051 (1990).

¹⁶C. Ambrosch-Draxl, P. Blaha, and K. Schwarz, *Phys. Rev. B* **44**, 5141 (1991).

¹⁷N. W. Winter, C. I. Merzbacher, and C. E. Violet, *Appl. Spectrosc. Rev.* **28**, 123 (1993).

¹⁸P. Hüsser, E. P. Stoll, H. U. Suter, and P. F. Meier, *Physica C* **294**, 217 (1998).

¹⁹H. U. Suter, E. P. Stoll, P. Hüsser, S. Schafroth, and P. F. Meier,

- Physica C **282-287**, 1639 (1997).
- ²⁰S. B. Sulaiman, N. Sahoo, T. P. Das, O. Donzelli, E. Torikai, and K. Nagamine, Phys. Rev. B **44**, 7028 (1991).
- ²¹R. L. Martin and P. J. Hay, J. Chem. Phys. **98**, 8680 (1993).
- ²²R. L. Martin, Phys. Rev. Lett. **75**, 744 (1995).
- ²³H. U. Suter, P. Hüsler, E. P. Stoll, S. Schafroth, and P. F. Meier, Hyperfine Interact. **121-121**, 137 (1999).
- ²⁴*Copper Oxide Superconductors*, Ch. P. Poole, T. Datta, and H. A. Farach (Wiley-Interscience, New York, 1988).
- ²⁵A. J. H. Wachters, J. Chem. Phys. **52**, 1033 (1970).
- ²⁶R. Krishnan, J. S. Binkley, R. Seeger, and J. A. Pople, J. Chem. Phys. **72**, 650 (1980).
- ²⁷M. J. Frisch *et al.*, GAUSSIAN 98, Revision A.5 (Gaussian, Inc., Pittsburgh, PA, 1998).
- ²⁸S. H. Vosko, L. Wilk, and M. Nussair, Can. J. Phys. **58**, 1200 (1980).
- ²⁹A. D. Becke, Phys. Rev. A **38**, 3098 (1988).
- ³⁰A. Becke, J. Chem. Phys. **88**, 2547 (1988).
- ³¹C. Lee, W. Yang, and R. G. Parr, Phys. Rev. B **37**, 785 (1988).
- ³²J. P. Perdew and W. Yang, Phys. Rev. B **45**, 13 244 (1992).
- ³³M. W. Schmidt, K. K. Baldrige, J. A. Boat, S. T. Elbert, M. S. Gordon, J. H. Jensen, S. Koseki, M. Matsunaga, K. A. Nguyen, S. J. Su, T. L. Windus, M. Dupuis, and J. A. Montgomery, J. Comput. Chem. **14**, 1347 (1993).
- ³⁴E. P. Stoll (unpublished).
- ³⁵T. Imai, C. P. Slichter, K. Yoshimura, and K. Kosuge, Phys. Rev. Lett. **70**, 1002 (1993).
- ³⁶B. Bleaney, K. D. Bowers, and M. H. L. Pryce, Proc. R. Soc. London, Ser. A **228**, 166 (1955).
- ³⁷W. E. Pickett, Rev. Mod. Phys. **61**, 433 (1989).
- ³⁸K. C. Hass, in *Solid State Physics: Advances in Research and Applications*, edited by D. Turnbull and H. Ehrenreich (Academic, New York, 1989), Vol. 42, p. 213.
- ³⁹R. M. Sternheimer, Z. Naturforsch. Teil A **41A**, 35 (1985).
- ⁴⁰J. Stein, S. B. Sulaiman, N. Sahoo, and T. P. Das, Hyperfine Interact. **60**, 849 (1990).
- ⁴¹K. Ishida, Y. Kitaoka, G.-Q. Zheng, and K. Asayama, J. Phys. Soc. Jpn. **60**, 3516 (1991).
- ⁴²V. Barone, in *Recent Advances in Density Functional Methods, Part I*, edited by D. P. Chong (World Scientific, Singapore, 1995).
- ⁴³V. Barone, J. Phys. Chem. **99**, 11 659 (1995).
- ⁴⁴V. Barone, R. Fournier, F. Mele, N. Russo, and C. Adamo, Chem. Phys. Lett. **237**, 189 (1995).
- ⁴⁵R. E. Walstedt, B. S. Shastry, and S-W. Cheong, Phys. Rev. Lett. **72**, 3610 (1994).
- ⁴⁶P. Hohenberg and W. Kohn, Phys. Rev. **136**, B864 (1964).
- ⁴⁷W. Kohn and L. J. Sham, Phys. Rev. **140**, A1133 (1965).
- ⁴⁸These effects have been studied in great detail for atoms and small molecules of light elements by quantum chemistry calculations [see, e.g., B. Engels and S. D. Peyerimhoff, J. Phys. B **21**, 3459 (1988)].
- ⁴⁹T. Imai, J. Phys. Soc. Jpn. **59**, 2508 (1990).